



1 Use of an Unmanned Aircraft System to Quantify NO_x Emissions 2 from a Natural Gas Boiler

3

4 Brian Gullett¹, Johanna Aurell², William Mitchell¹, Jennifer Richardson³

5

6 ¹US Environmental Protection Agency, Office of Research and Development, Research Triangle Park, North
7 Carolina, 27711, USA; ²University of Dayton Research Institute, Dayton, Ohio, 45469-7532, USA; ³The Dow
8 Chemical Company, Midland, Michigan, 48667, USA.

9 *Correspondence to:* Brian Gullett (gullett.brian@epa.gov)

10

11 Abstract

12 Aerial emission sampling of four natural gas boiler stack plumes was conducted using an unmanned aerial system
13 (UAS) equipped with a light-weight sensor/sampling system (the “Kolibri”) for measurement of nitrogen oxide
14 (NO), and nitrogen dioxide (NO₂), carbon dioxide (CO₂), and carbon monoxide (CO). Flights (n = 22) ranged from
15 11 to 24 minutes duration at two different sites. The UAS was maneuvered into the plumes with the aid of real-time
16 CO₂ telemetry to the ground operators and, at one location, a second UAS equipped with an infrared/visible camera.
17 Concentrations were collected and recorded at 1 Hz. The maximum CO₂, CO, NO, and NO₂ concentrations in the
18 plume measured were 10,000 ppm, 7 ppm, 27 ppm, and 1.5 ppm, respectively. Comparison of the NO_x emissions
19 between the stack continuous emission monitoring systems and the UAS/Kolibri for three boiler sets showed an
20 average of 5.6 % and 3.5 % relative percent difference for the run-weighted and carbon-weighted average emissions,
21 respectively.

22 **Keywords:** Emissions, natural gas, boiler, unmanned aircraft system, drone, continuous emission monitoring



23

24 TOC Art

25



26 1 Introduction

27 Aerial measurement of plume concentrations is a new field made possible by advances in Unmanned Aircraft
28 Systems (UAS, or “drones”), miniature sensors, computers, and small batteries. The use of a UAS platform for
29 environmental sampling has significant advantages in many scenarios in which access to environmental samples are
30 limited by location or accessibility. Hazards to equipment and personnel can also be minimized by the mobility of
31 the UAS as well as their ability to be remotely operated away from hazardous sources. UAS-based emission
32 samplers have been used for measurement of area source gases (Neumann et al., 2013; Rosser et al., 2015; Chang et
33 al., 2016; Li et al., 2018), point source gases (Villa et al., 2016), aerosols (Brady et al., 2016), black carbon particles
34 (Craft, 2014), volcanic pollutants (Mori et al., 2016), particle mass (Peng et al., 2015), and particle number
35 concentrations (Villa et al., 2016).

36 UAS-based emission measurements are particularly suited for area source measurements of fires and can be used to
37 determine emission factors, or the mass amount of a pollutant per unit of source operation, such as mass of
38 particulate matter (PM) per mass of fuel (e.g., biomass) burned. These values can be converted into emission rates,
39 such as mass of pollutant per unit of energy (e.g., $\text{g NO}_x \text{ kJ}^{-1}$). These determinations typically rely on the carbon
40 balance method in which the target pollutant is co-sampled with the major carbon species present and, with
41 knowledge of the source’s fuel (carbon) composition, the pollutant to fuel ratio or an emission rate/factor, can be
42 calculated.

43 For internal combustion sources that have a process emission stack, downwind plume sampling can use the same
44 method. When combined with the source fuel supply rate and stack flow rates (to determine the dilution rate),
45 measurements comparable to extractive stack sampling may be possible. To our knowledge, determination of
46 emission factors from a stack plume using a UAS-borne sampling system has not previously been demonstrated.

47 The feasibility of downwind plume sampling using a sensor-equipped UAS was tested on industrial boilers at the
48 Dow Chemical Company (Dow) facilities in Midland, Michigan (MI) and St. Charles, Louisiana (LA). The sensor
49 system was designed and built by the EPA’s Office of Research and Development and the UAS was owned and
50 flown by the Dow Corporate Aviation Group. To determine the comparative accuracy of the measurements, the
51 UAS-based emission factor was compared with the stack continuous emission monitoring systems (CEMS). The
52 target pollutants were nitrogen oxide (NO) and nitrogen dioxide (NO₂) to mimic the stack CEMS measurement
53 methods. Carbon as carbon dioxide (CO₂) and carbon monoxide (CO) were measured on the UAS for the carbon
54 balance method.

55 2 Materials and Method

56 Plume sampling tests were conducted on two natural-gas-fired industrial boilers located at Dow’s Midland,
57 Michigan and St. Charles, Louisiana facilities. The Midland boilers are firetube type boilers using low pressure
58 utility supplied natural gas. They are equipped with low NO_x burners and utilize flue gas recirculation to reduce
59 stack NO_x concentrations. The Midland facility burned natural gas with a higher heating value (HHV) of 9,697 kcal
60 m^{-3} (1089 British Thermal Unit (BTU)/ft³). The two tested stacks are 14 m above ground level and 7 m apart. To
61 avoid sampling overlapping plumes, only a single boiler was operating during the testing. The St. Charles boilers are
62 D-type water package boilers using natural gas fuels (high pressure fuel gas (HPFG) and low pressure off-gas
63 (LPOG)). They are equipped with low NO_x burners with flue gas recirculation to reduce stack NO_x concentrations.
64 The boiler stacks are about 20 m apart and reach over 20 m in height above ground level. The St. Charles facility
65 burned natural gas under steady state conditions with a composition of 77.12 % CH₄, 2.01 % C₂H₆, and 19.91 % H₂
66 and a HHV of 7,845 kcal m^{-3} (881 BTU ft³). Both boilers were operational during aerial sampling, but the wind
67 direction and UAS proximity to the target stack precluded co-mingling of the plumes.



68 Air sampling was accomplished with an EPA/ORD-developed sensor/sampler system termed the “Kolibri”. The
69 Kolibri consists of real-time gas sensors and pump samplers to characterize a broad range of gaseous and particle
70 pollutants. This self-powered system has a transceiver for data transmission and pump control (Xbee S3B, Digi
71 International, Inc., Minnetonka, MN, USA) from the ground-based operator. For this application, gas concentrations
72 were measured using electrochemical cells for CO, NO, and NO₂ and a non-dispersive infrared (NDIR) cell for CO₂
73 (Table 1). All sensors were selected for their applicability to the anticipated operating conditions of concentration
74 level and temperature as well as for their ability to rapidly respond to changing plume concentrations due to
75 turbulence and entrainment of ambient air. Each sensor underwent extensive laboratory testing to verify
76 performance and suitability prior to selection for the Kolibri. In anticipation of temperatures as low as 0°C at the
77 Midland site, insulation was added to the Kolibri frame and the sampled gases were preheated prior to the sensor
78 with the use of a heating element and micro fan inside the Kolibri.

79 Concentration data were stored by the Kolibri using a Teensy USB-based microcontroller board (Teensy 3.2, PJRC,
80 LLC., Sherwood, OR, USA) with an Arduino-generated data program and SD data card. All four sensors underwent
81 pre- and post-sampling two- or three-point calibration using gases (Calgasdirect Inc., Huntington Beach, CA, USA)
82 traceable to National Institute of Standards and Technology (NIST) standards.

83
84
85

Table 1. UAS/Kolibri Target Analytes and Methods

Analyte	Instrument	Frequency	Cal. Gases	Cal Gases (ppm)
			(ppm)	LA
			Midland	
CO ₂	SenseAir CO ₂ Engine K30, NDIR ^a	Continuous, 1 Hz ^b	408, 990	392, 996, 5890
CO	E2v EC4-500-CO, Electrochemical cell	Continuous, 1 Hz	0 ^c , 9.67, 50.6	0, 9.9, 51.8
NO	NO-D4, Electrochemical cell	Continuous, 1 Hz	0, 2.1, 41.4	0, 2.1, 40.4
NO ₂	NO ₂ -D4, Electrochemical cell	Continuous, 1 Hz	0, 2.1, 10.4	0, 1.9, 10.4

86 ^aNon-dispersive infrared. ^bHz – hertz. ^cZero (0) cal gas = air.

87

88 The NO sensor (NO-D4) is an electrochemical gas sensor (Alphasense, Essex, UK) which measures concentration
89 by changes in impedance. The sensor has a detection range of 0 to 100 ppm with resolution of < 0.1 RMS noise
90 (ppm equivalent) and linearity within ±1.5 ppm error at full scale. The NO-D4 was tested to have a response time to
91 95 % of concentration (T_{95%}) of 6.3±0.52 seconds and a noise level of 0.027 ppm. The temperature and relative
92 humidity (RH) operating range is 0 to +50 °C and 15 to 90 % RH, respectively.

93 The NO₂ sensor (NO₂-D4) is an electrochemical gas sensor (Alphasense, Essex, UK) which likewise measures by
94 impedance changes. It has a NO₂ detection range of 0-10 ppm with resolution of 0.1 RMS noise (ppm equivalent)
95 and linearity error of 0 to 0.6 ppm at full scale. Its T_{95%} was measured as 32.3±3.8 seconds with a noise level of
96 0.015 ppm. The temperature and RH operating range is 0 to +50 °C and 15 to 90 % RH, respectively.

97 The CO₂ sensor (CO₂ Engine® K30 Fast Response, SenseAir, Delsbo, Sweden) is a NDIR gas sensor and the
98 voltage output is linear from 400 to 10,000 ppm. The temperature and RH operating range is 0 to +50 °C and 0 to 90
99 % RH, respectively. The CO₂-K30 sensor was measured to have a T_{95%} response time at 6000 ppm CO₂ of 9.0 ± 0.0
100 seconds and having a noise level of 1.6 ppm.



101 The CO sensor (e2V EC4-500-CO, SGX Sensortech Ltd, High Wycombe, Buckinghamshire UK) is described more
102 fully elsewhere (Aurell et al., 2017; Zhou et al., 2017). Variations of the Kolibri sampling system allow for
103 measurement of additional target pollutants including particulate matter (PM), polycyclic aromatic hydrocarbons
104 (PAHs), volatile organic compounds (VOCs) including carbonyls, energetics, chlorinated organics, and perchlorate
105 (Aurell et al., 2017; Zhou et al., 2017).

106 At both facilities the aviation team from Dow flew their DJI Matrice 600 UAS, a six-motor multicopter
107 (hexacopter), into the plumes with EPA/ORD's Kolibri sensor/sampler system attached to the undercarriage (Figure
108 1). In this configuration of sensors, the Kolibri system weighed 2.4 kg. Typical flight elevations at Midland and St.
109 Charles were 21 and 32 m above ground level (AGL), respectively, and flight durations ranged from 9 to 24 min.
110 At the St. Charles location, the UAS pilot was approximately 100 m from the center point of the two stacks, easily
111 allowing for line of sight operation. A telemetry system on the Kolibri provided real time CO₂ concentration and
112 temperature data to the Kolibri operator who in turn advised the pilot on the optimum UAS location.

113 CEMS on the boiler stacks produced a continuous record of NO_x emission and O₂ concentrations. Stack and CEMS
114 types located at the Midland and St. Charles facilities are shown in Table 2. The stack NO_x analyzer is capable of
115 split concentration range operation: Low (0-180 ppm) and High (0-500 ppm).



116
117 **Figure 1. Dow UAS with Kolibri attached to the undercarriage.**

118
119 **Table 2. CEMS Instruments at both Dow locations.**

Gas Measured	Midland CEMS	St. Charles CEMS
O ₂	Gaus Model 4705	ABB/Magnos 106
NO _x	Thermo Model 42i-HL	ABB/Limas 11

120
121 The plant CEMS undergo annual relative accuracy audit testing (NSPS Subpart Db, Part 70) using EPA Method 7E
122 (2014) for NO_x and Method 3A (2017a) for O₂. Calculation of NO_x emissions use the appropriate F factor, a value



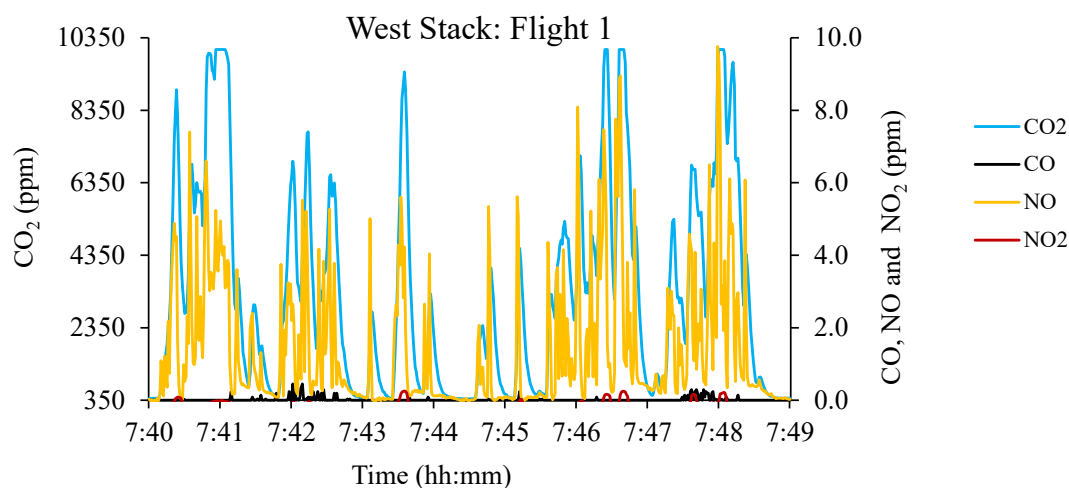
123 that relates the required combustion gas volume to fuel energy input, as described in EPA Method 19 (2017b). Flue
124 gas analysis for O₂ and CO₂ are performed in accordance with Method 3A (2017a) using an infrared analyzer to
125 allow for calculation of the flue gas dry molecular weight.

126 The CEMS and UAS/Kolibri data were reduced to a common basis for comparison of results. Emission factors, or
127 mass of NO_x per mass of fuel carbon burned, and emission rates, or mass of NO_x per energy content of the fuel,
128 were calculated from the sample results. The determination of emission factors, mass of pollutant per mass of fuel
129 burned, depends upon foreknowledge of the fuel composition, specifically its carbon concentration, and its supply
130 rate. The carbon in the fuel is presumed for calculation purposes to proceed to either CO₂ or CO, with the minor
131 carbon mass in hydrocarbons and PM ignored for this source type. Concurrent emission measurements of pollutant
132 mass and carbon mass (as CO₂ + CO) can be used to calculate total emissions of the pollutant from the fuel using its
133 carbon concentration and fuel burn rate.

134 The UAS/Kolibri emission factors were calculated from the mass ratio of NO + NO₂ with the mass of CO + CO₂
135 resulting in a value with units of mg NO_x kg⁻¹ C. CO₂ concentrations were corrected for upwind background
136 concentrations. CEMS values of O₂ and fuel flowrate were used to calculate stack flowrate using US EPA Method
137 19 (2017b). This Method requires the fuel higher heating value and an F factor (gas volume per fuel energy content,
138 e.g., m³ kcal⁻¹ (ft³ BTU⁻¹)) to complete this calculation. For natural gas, the F factor is 967 m³ 10⁻⁶ kcal (8,710 ft³ 10⁻⁶
139 BTU) (Table 19-2, EPA Method 19 (2017b)). The concentration, stack flowrate, and fuel flowrate data allow
140 determination of NO_x and C emission rates.

141 3 Results and Discussion

142 The UAS/Kolibri team easily found the stack plumes at both locations using the wind direction and CO₂ telemetry
143 data transmitted to the ground operator. Use of an infra-red (IR)/visible camera on a second UAS at St. Charles for
144 some of the flights aided more rapid location of the plume and positioning of the UAS/Kolibri. Gas concentration
145 fluctuations were rapid and of high magnitude as observed in a representative trace in Figure 2. CO₂ concentrations
146 to 10,000 ppm were observed; the relatively lower average CO₂ concentrations reflect the rapid mixing and
147 entrainment of ambient air causing dilution.



148

149 **Figure 2.** Example of UAS/Kolibri-measured plume concentrations from the St. Charles West Boiler.



150 Sampling data and emission factors from the UAS/Kolibri are shown in Tables 3, 4, and 5 for the Midland, St.
 151 Charles east stack, and St. Charles west stack, respectively. Eight sampling flights were conducted at the Midland
 152 site, five on the St. Charles East boiler, and nine on the St. Charles West boiler. Both boilers at the Midland site
 153 were operated under the same conditions, so their results have been presented together. Flights averaged 14 min (10
 154 % relative standard deviation (RSD)) at the Midland facility and just over 20 min (10 % RSD) at the St. Charles
 155 facility. The shorter flight times in Midland were due to lower UAS battery capacity caused by colder temperatures
 156 (the sampling temperatures in the plume averaged $10\pm 3^{\circ}\text{C}$). Average plume NO_x concentrations were 0.88 ± 0.32
 157 ppm at Midland and 1.22 ppm and 2.41 ppm at the two St. Charles boilers with an average RSD of 37 %, 36 %, and
 158 12 %, respectively. The NO emission factor was typically 97 % of the total NO_x , with the NO_2 providing the minor
 159 balance.

160

161 **Table 3. Midland UAS/Kolibri Sampling Data and Emission Factors.**

Date	Flight #	Flight time (hh:mm:ss)			NO_2 mg kg ⁻¹ C	NO mg kg ⁻¹ C	NO_x mg kg ⁻¹ C	Avg. CO_2 ppm
		Up	Down	Total				
11/14/2018	1	10:29:00	10:43:00	00:14:00	201	618	819	1213
11/14/2018	2	11:13:04	11:28:28	00:15:24	186	624	810	1138
11/14/2018	3	12:54:17	13:08:47	00:14:30	230	659	889	2948
11/14/2018	5	13:27:40	13:42:05	00:14:25	99	570	669	4658
11/15/2018	6	10:24:20	10:39:30	00:15:10	61	394	454	3703
11/15/2018	7	10:41:36	10:52:40	00:11:04	84	397	481	3983
11/15/2018	8	10:55:10	11:10:10	00:15:00	126	398	524	4781
Average				00:14:13	141	523	664	3203
Stand. Dev.				00:01:28	65	121	179	1514
RSD (%)				10	46	23	27	47

162 Flight # 4 excluded from calculations as CO was observed, which originated from a cycling second boiler.

163

164 **Table 4. St. Charles East Stack UAS/Kolibri Sampling Data and Emission Factors.**

Date	Flight #	Flight time (hh:mm:ss)			NO_2 mg kg ⁻¹ C	NO mg kg ⁻¹ C	NO_x mg kg ⁻¹ C	Avg. CO_2 ppm
		Up	Down	Total				
07/23/2019	1	09:49:00	10:07:00	00:18:00	1	1442	1442	2305
07/23/2019	2	10:12:00	10:34:00	00:22:00	15	1461	1476	2526
07/23/2019	3	10:45:00	11:08:00	00:23:00	5	1534	1539	785
07/23/2019	4	11:11:00	11:31:00	00:20:00	101	1684	1785	1082
07/23/2019	5	11:52:00	12:01:00	00:09:00	107	2110	2217	1923
Average				00:20:45	30	1530	1560	1675
Stand. Dev.				00:02:13	47	110	155	869
RSD (%)				11	155	7.2	9.9	52

165 *Flight # 5 was not included in the average as elevated CO concentrations were detected, likely from other sources*
 166 *in the facility.*



167 **Table 5. St. Charles West Stack UAS/Kolibri Sampling Data and Emission Factors.**

Date	Flight #	Flight time (hh:mm:ss)			NO ₂ mg kg ⁻¹ C	NO mg kg ⁻¹ C	NO _x mg kg ⁻¹ C	Avg. CO ₂ ppm
		Up	Down	Total				
07/24/2019	1	07:31:00	07:49:00	00:18:00	25	1366	3221	1490
07/24/2019	2	07:52:00	08:16:00	00:24:00	49	1263	3503	1397
07/24/2019	3	08:19:00	08:38:00	00:19:00	87	1420	3415	1611
07/24/2019	4	09:23:00	09:46:00	00:23:00	65	1341	4509	1525
07/24/2019	5	09:49:00	10:11:00	00:22:00	47	1296	4813	1463
07/24/2019	6	10:16:00	10:36:00	00:20:00	52	1299	3773	1449
07/24/2019	7	10:38:00	11:00:00	00:22:00	53	1316	4194	1482
07/24/2019	8	11:51:00	12:13:00	00:22:00	90	1460	3129	1662
07/24/2019	9	13:17:00	13:39:00	00:22:00	47	1464	3606	1645
Average				00:21:20	57	1358	1416	3796
Stand. Dev.				00:01:56	21	74	86	586
RSD (%)				9	36	5.5	6.0	15

168

169 Table 6 presents the average O₂ and NO_x measurement results and the fuel supply rate at both locations. Values for
 170 natural gas supply, adjusted for the C₂H₆ and H₂ composition of the St. Charles fuel, were used to calculate the fuel
 171 carbon supply rate. These data allow calculation of the emission factor, mass of NO_x to the mass of carbon, reported
 172 in Table 7.

173

174 **Table 6. Multi-Run Average Stack CEMS Data**

	Midland	St. Charles	
	Both Boilers	East Boiler	West Boiler
O ₂ (%)	8.2	4.9	4.5
NO _x (ppm)	15.7	50.4	42.9
Fuel rate	39.3 10 ⁶ kJ h ⁻¹	155.2 10 ⁶ kJ h ⁻¹	177.8 10 ⁶ kJ h ⁻¹

175

176 **Table 7. Comparison of Average NO_x Emission Factors from CEMS and UAS/Kolibri**

	Run-Averaged NO _x Emission Factor, mg NO _x kg ⁻¹ C (± 1 std dev)		
	Midland	St. Charles	
	Both Boilers	East Boiler	West Boiler
CEMS	612 ± 10	1555 ± 50	1303 ± 29
UAS/Kolibri	664 ± 179	1560 ± 155	1416 ± 86
RPD: CEM & UAS/Kolibri, %	8.2	0.3	8.3



177 The UAS/Kolibri NO_x emission factor for Midland is 8 % higher than the simultaneous CEMS value. For the East
178 and West boilers at St. Charles, the UAS/Kolibri NO_x emission factor value is <1 % and 8 % higher, respectively,
179 than the CEMS values. The difference for the UAS/Kolibri in Midland may be attributed in part to the extremely
180 cold temperature affecting the performance of the electrochemical sensors. The standard deviations for the CEMS
181 data are based on the run-average NO_x values for each test. These values were calculated based on 10 sec averaging
182 for the Midland tests, 60 sec averaging in St. Charles, and 1 sec averaging for the UAS/Kolibri. Higher standard
183 deviations for the UAS/Kolibri are predictable given the rapidly changing values and wide range (~0-10 ppm) of
184 NO_x data observed in Figure 2. Difference testing for the CEMS and UAS/Kolibri using $\alpha = 0.05$ and assumed
185 unequal variances indicate that only the West Boiler and UAS/Kolibri are statistically distinct.

186 The emission rates calculated from the UAS/Kolibri data are $5.6 \text{ kg NO}_x \cdot 10^{-3} \text{ kJ}$, $14.6 \text{ kg NO}_x \cdot 10^{-3} \text{ kJ}$, and 13.3 kg
187 $\text{NO}_x \cdot 10^{-3} \text{ kJ}$ (0.013, 0.034, and 0.031 lbs $\text{NO}_x \cdot 10^{-6} \text{ BTU}$), respectively, for the Midland, East St. Charles, and West
188 St. Charles boilers, below the regulatory standard of $15.5 \text{ kg NO}_x \cdot 10^{-3} \text{ kJ}$ (0.036 lbs $\text{NO}_x \cdot 10^{-6} \text{ BTU}$). The emission
189 factors were also calculated as carbon-weighted values to reflect potential differences in plume sampling efficiency
190 between runs. The Midland, East St. Charles, and West St. Charles UAS/Kolibri emission factors were, respectively,
191 607, 1525, and 1409 $\text{mg NO}_x \text{ kg}^{-1} \text{ C}$. These amounted to relative percent differences of 0.8, 1.9, and 7.8 % between
192 the CEM and UAS/Kolibri values, for an overall run-weighted average difference of 5.6 %. The difference between
193 the CEM readings and those from the Kolibri weighted by the carbon collection amounts, reflecting the success at
194 being within the higher plume concentrations, was 3.5 %.

195

196 **4 Conclusions**

197 This work reports, to our knowledge, the first known comparison of continuous emission monitoring measurements
198 made in a stack with downwind plume measurements made using a UAS equipped with emission sensors.

199 The UAS/Kolibri system was easily able to find and take measurements from the downwind plume of a natural gas
200 boiler despite lack of any visible plume signature. The telemetry system aboard the Kolibri system reported real time
201 CO_2 concentrations to the operator on the ground, allowing the operator to provide immediate feedback to the UAS
202 pilot on plume location. Comparison of the CEM data with the UAS/Kolibri data from field measurements at two
203 locations showed agreement of NO_x emission factors within 5.6 % and 3.5 % for time-weighted and carbon-
204 collection-weighted measurements, respectively.

205

206 Data availability. The tabular and figure data are available at the Environmental Dataset Gateway
207 <https://edg.epa.gov/metadata/catalog/main/home.page>.

208

209 Author contributions. BG was the prime author of the paper and the project lead. JA conducted the Kolibri field
210 testing and data analysis. WM designed the instrument electronics. JR led the UAS group and field test
211 arrangements.

212

213 Competing interests. The authors declare that they have no conflict of interest.

214



215 Disclaimer. The views expressed in this article are those of the authors and do not necessarily represent the views or
216 policies of the U.S. EPA.
217

218 Acknowledgements. Dow's Corporate Aviation Group: Laine Miller, Bryce Young, James Waddell, Jeffrey
219 Matthews, Chris Simmons, and Anthony DiBiase conducted flights flawlessly. Dow employees Rob Seibert and
220 Alex Kidd provided technical data and Amy Meskill (Dow), Jennifer DeMelo (Dow), and Dale Greenwell
221 (EPA/ORD) provided critical logistic support. Patrick Clark (Montrose) reviewed the St. Charles CEMS data.

222
223 Financial support. This work was supported through a Cooperative Research and Development Agreement between
224 the U.S. EPA and The Dow Chemical Company.
225
226
227

228 References

- 229 Aurell, J., W. Mitchell, V. Chirayath, J. Jonsson, D. Tabor, and B. Gullett. 2017. Field determination of
230 multipollutant, open area combustion source emission factors with a hexacopter unmanned aerial vehicle.
231 *Atmospheric Environment* **166**:433-440.
- 232 Brady, J. M., M. D. Stokes, J. Bonnardel, and T. H. Bertram. 2016. Characterization of a Quadrotor Unmanned
233 Aircraft System for Aerosol-Particle-Concentration Measurements. *Environmental Science & Technology*
234 **50**:1376-1383.
- 235 Chang, C.-C., J.-L. Wang, C.-Y. Chang, M.-C. Liang, and M.-R. Lin. 2016. Development of a multicopter-carried
236 whole air sampling apparatus and its applications in environmental studies. *Chemosphere* **144**:484-492.
- 237 Craft, T. L. C., C.F.; Walker, G.W. 2014. Using an Unmanned Aircraft to Observe Black Carbon Aerosols During a
238 Prescribed Fire at the RxCADRE Campaign. 2014 International Conference on Unmanned Aircraft
239 Systems **May 27-30, 2014**.
- 240 Li, X. B., D. F. Wang, Q. C. Lu, Z. R. Peng, Q. Y. Fu, X. M. Hu, J. T. Huo, G. L. Xiu, B. Li, C. Li, D. S. Wang, and
241 H. Y. Wang. 2018. Three-dimensional analysis of ozone and PM_{2.5} distributions obtained by observations
242 of tethered balloon and unmanned aerial vehicle in Shanghai, China. *Stochastic Environmental Research
243 and Risk Assessment* **32**:1189-1203.
- 244 Mori, T., T. Hashimoto, A. Terada, M. Yoshimoto, R. Kazahaya, H. Shinohara, and R. Tanaka. 2016. Volcanic
245 plume measurements using a UAV for the 2014 Mt. Ontake eruption. *Earth Planets and Space* **68**:18.
- 246 Neumann, P. P., V. H. Bennetts, A. J. Lilienthal, M. Bartholmai, and J. H. Schiller. 2013. Gas source localization
247 with a micro-drone using bio-inspired and particle filter-based algorithms. *Advanced Robotics* **27**:725-738.
- 248 Peng, Z.-R., D. Wang, Z. Wang, Y. Gao, and S. Lu. 2015. A study of vertical distribution patterns of PM_{2.5}
249 concentrations based on ambient monitoring with unmanned aerial vehicles: A case in Hangzhou, China.
250 *Atmospheric Environment* **123**:357-369.
- 251 Rosser, K., K. Pavey, N. FitzGerald, A. Fatiaki, D. Neumann, D. Carr, B. Hanlon, and J. Chahl. 2015. Autonomous
252 Chemical Vapour Detection by Micro UAV. *Remote Sensing* **7**:16865-16882.
- 253 U.S. EPA Method 7E. 2014. Determination of Nitrogen Oxides Emissions from Stationary Sources (Instrumental
254 Analyzer Procedure). <https://www.epa.gov/sites/production/files/2016-06/documents/method7e.pdf>
255 Accessed August 7, 2019
- 256 U.S. EPA Method 3A. 2017a. Determination of oxygen and carbon dioxide concentrations in emissions from
257 stationary sources (instrumental analyzer procedure). [https://www.epa.gov/sites/production/files/2017-
258 08/documents/method_3a.pdf](https://www.epa.gov/sites/production/files/2017-08/documents/method_3a.pdf) Accessed February 12, 2019



- 259 U.S. EPA Method 19. 2017b. Determination of sulfur dioxide removal efficiency and particulate matter, sulfur
260 dioxide, and nitrogen oxide emission rates. [https://www.epa.gov/sites/production/files/2017-](https://www.epa.gov/sites/production/files/2017-08/documents/method_19.pdf)
261 [08/documents/method_19.pdf](https://www.epa.gov/sites/production/files/2017-08/documents/method_19.pdf) Accessed December 6, 2018
- 262 Villa, T. F., F. Salimi, K. Morton, L. Morawska, and F. Gonzalez. 2016. Development and Validation of a UAV
263 Based System for Air Pollution Measurements. *Sensors* **16**.
- 264 Zhou, X., J. Aurell, W. Mitchell, D. Tabor, and B. Gullett. 2017. A small, lightweight multipollutant sensor system
265 for ground-mobile and aerial emission sampling from open area sources. *Atm. Env.* **154**:31-41.